

## **Computational and Experimental Analysis of Acetabular Reinforcement Devices**

P. M. A. Talaia<sup>1</sup>, C. Relvas<sup>1</sup>, L. Almeida<sup>2</sup>, J. Salgado<sup>2</sup>, J. A. Simões<sup>1</sup>

### **Summary**

This paper describes the design of a device to perform static and dynamical tests of Acetabular Reinforcement Devices (ARDs), which are similar to the Kerboul acetabular reinforcement used in major acetabular reconstructions. The device was designed based on preliminary computational simulations and experimental mechanical testing was performed on ARDs. The suitability of the testing device and results are presented and discussed.

### **Introduction**

Severe aseptic acetabular deficiencies can be treated with bulk allograft bone and the Kerboul acetabular reinforcement device. In a study performed by Hamadouche and Kerboul [1,2], acetabular allograft reconstructions reinforced by the Kerboul acetabular device were able to provide satisfactory long-term clinical and radiological results. Other methods, for example, comprise wire mesh, the Eichler or Müller ring [3], or a combination of both. As for these methods, both mesh and Eichler ring increase load-bearing capacity by 75 per cent. However, it seems that the combination of both systems can increase the load-bearing capacity in a further 45 per cent in the medial support. Wire mesh provides suitable support for patients with mild or moderate protrusion; the Eichler ring solely is excellent for pillar deficiency. For cases of severe protrusion with pillar deficiency, the combination of Eichler ring and wire mesh is the best implant. The objective of the work discussed here was to design and test a device to determine the resistance mechanical properties of similar Kerboul ARDs.

### **Materials and Methods**

Due to the inexistence of standardization concerning these types of orthopedic devices, the design of a test rig was done to perform mechanical testing. The geometrical and dimensional characteristics of the device were defined based on numerical analysis, previously realized. Stiffness properties of the device were considered as the critical project parameter and it should be designed in order to not compromise its resistance, and should not influence the testing and results of the ARD. The numerical simulations gave the necessary output data, namely the maximum vertical displacement before fracture

---

<sup>1</sup> Departamento de Engenharia Mecânica, Universidade de Aveiro, Portugal

<sup>2</sup> L. A. Medical, Fabricantes de Instrumentos Cirúrgicos Lda, Albergaria-a-Velha, Portugal

(direction of the tensile force) and the ultimate load. Figure 1 shows the CAD model of the ARD manufactured and tested, while figure 2 shows a perspective of the test rig.



Figure 1 – CAD model of the Acetabular Reinforcement Device.

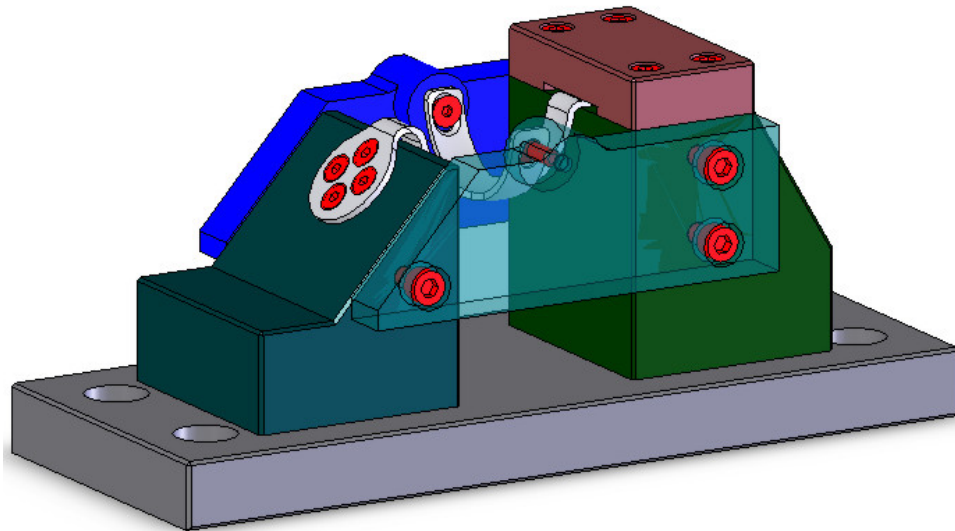


Figure 2 – Assembly of the test device.

The rig comprises a base that is fixed to a universal testing machine by 4 screws. The fixation of the ARD is obtained through four M5 screws. The opposite arm to the fixation one was held by friction and its vertical displacement restrained, although it allowed the slipping of the arm. The device was designed to allow the necessary testing flexibility concerning fixation conditions of the ARD.

### Computational Analysis

The stress-strain fields of testing device have been determined through extensive numerical simulations using the finite element method, where the fracture load of the ARD was estimated. A force of 10000N was applied and titanium material (Elastic modulus = 110 GPa, Poisson's ratio = 0.3; Yield Strength = 140 MPa and Ultimate Tensile Strength = 245 MPa) was assigned to the material of the device. The loading and fixation conditions were similar to the mechanical testing, although it was not possible to simulate the slipping effect of the arm due to software limitations, which were performed with CosmosWorks®.

Figure 3 shows the finite element mesh (tetrahedral linear elements) and the equivalent von Mises stress distribution. The region of the highest stress gradient, and therefore the regions of higher probability of implant failure, were assessed. Mechanical testing confirmed these findings.

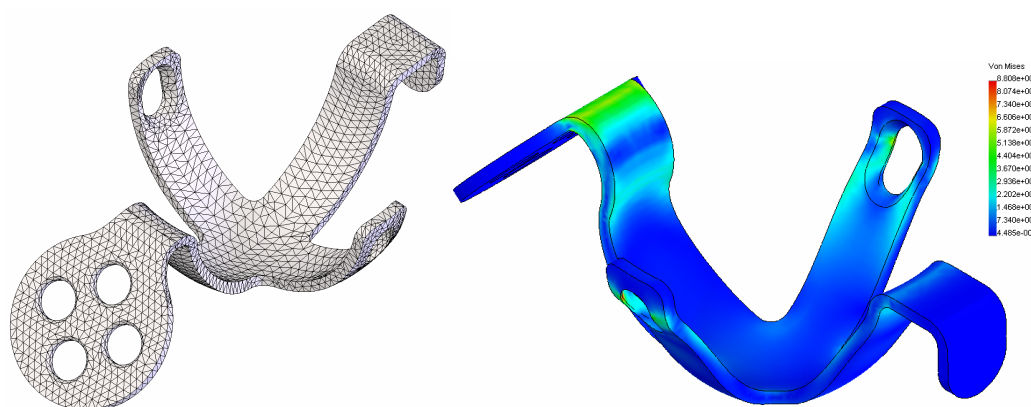


Figure 3 – Finite elements mesh and von Mises stress distribution.

The numerical simulations of the device designed showed that the stress levels are significantly low and the strain distribution apparently will not influence the stiffness and resistance properties of the ARDs. All parts of the device were machined in F10 steel (F. Ramada). Figure 4 shows the device manufactured.

### Mechanical testing

Three tests were performed in order to characterize the mechanical behaviour of titanium ARDs using a universal testing machine. Two of the ARD's tested were fixed by the "ear" using four M5 screws and the other two opposite side arms were held with M5 screws. The other arm was able to slide, but was vertically restrained. One ARD was

tested in the same way, but the arm opposite to the “ear” arm was not restrained. All ARD’s tested were placed on the vertical axis of the machine direction, loading them through a sphere at a testing speed of 15m/s.

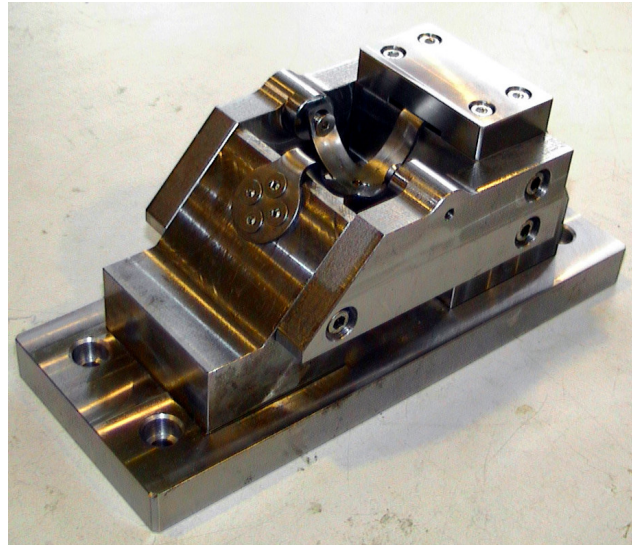


Figure 4 – Device for mechanical testing of ARDs.

### Results and Discussion

Figure 5 shows the force-displacement graphs of the tests performed and it can be seen that the ARDs with sliding arm free can sustain a load around 10000 kN; if the sliding arm is vertically restrained, the implant can sustain a load higher than 15000 N before fracture.

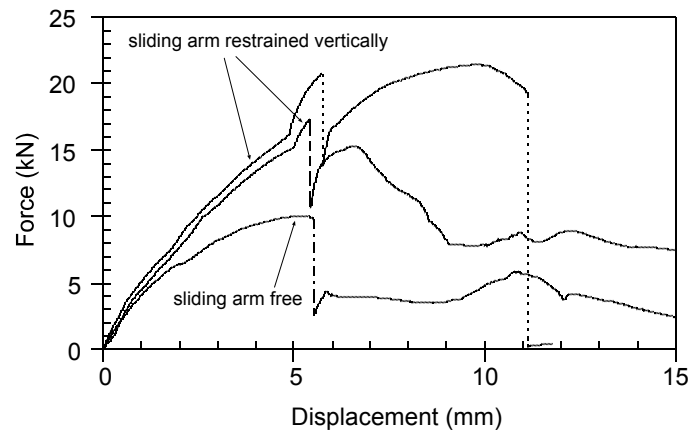


Figure 5 – Graphic Force (kN)-Displacement (mm) of the tests performed.

The force-displacement results show that ARDs collapse due to mainly plastic deformation. In all tests performed, fracture always occurred in one of the arms fixed with the screw (figure 6). The fracture in this precise region of the ARD was also predicted by the numerical results (see figure 3). The second instant of fractures occurred in the ARDs “ear” arm. The fracture of the “ear” after the first fracture was predicted numerically. Figure 7 illustrates the fracture of one of the ARD tested.

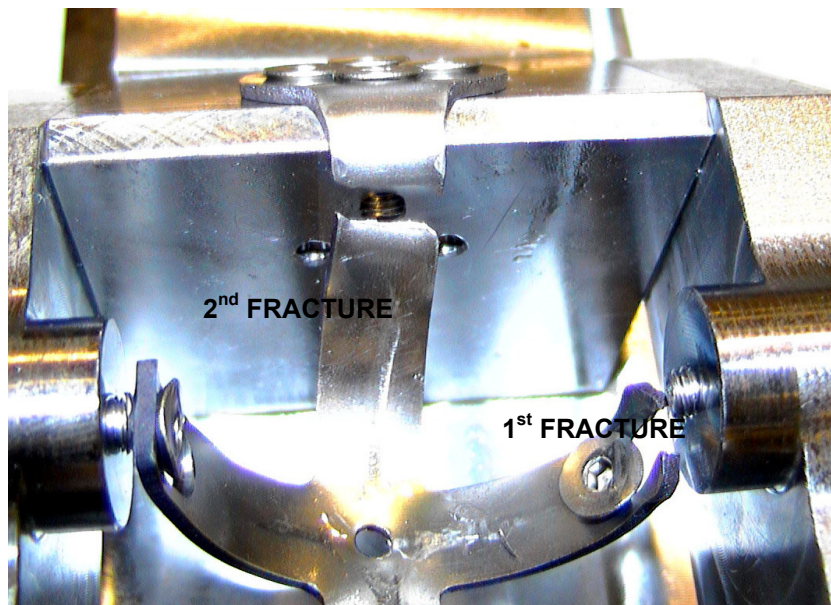


Figure 6 – Typical fracture of the ARDs simulated.

### Conclusions

The design and structural computational of the test device allowed the determination of the stress-strain distribution that ARDs are theoretically subjected too. The device designed and used within the mechanical testing presents adequate stiffness and resistance properties to perform static and fatigue tests, although no ARD was tested dynamically.

The tests performed allowed to determine the maximum force, under tension, that an ARD can support, which was of the order of 10 000N. We must recall the attention to the fact that the specimens were tested in a much more adverse condition than an *in vivo* situation.



Figure 5 – Fracture of an ARD after testing.

### References

- 1 Kerboull, M., Hamadouche, M. and Kerboull, L. (2000): “The Kerboull acetabular reinforcement device in major acetabular reconstructions”, *Clin Orthop*, 378, pp. 155-168.
- 2 Kerboull, M., Hamadouche, M. and Kerboull, L. (2001): “The Kerboull acetabular reinforcement device in major acetabular reconstructions”, *Am Acad of Orthop Surg*, Feb 28 – Mar 4, San Francisco, CA.
- 3 Herentjens, P., De Boeck, H., Handelberg, F., Kerboull, L. et al., (1991): “Cemented acetabular reconstruction with the Müller support ring”, *Clin Orthop*, 290, pp. 225-235.